now appeared in J.Chem.Phys., 131, 174107.1-6 (2009)

A soft–core Gay–Berne model for the simulation of liquid crystals by Hamiltonian replica exchange

Roberto Berardi and Claudio Zannoni

Dipartimento di Chimica Fisica e Inorganica,

Università di Bologna and INSTM, viale Risorgimento 4, 40136 Bologna, IT

Juho S. Lintuvuori and Mark R. Wilson,

Department of Chemistry,

Durham University, South Road, Durham, DH1 3LE, UK

[version Monday, September 14, 2009]

Abstract

The Gay–Berne (GB) potential has proved highly successful in the simulation of liquid crystal phases, although it is fairly demanding in terms of resources for simulations of large (*e.g.* $N > 10^5$) systems, as increasingly required in applications. Here we introduce a soft-core GB model, which exhibits both liquid crystal phase behaviour and rapid equilibration. We show that the Hamiltonian replica exchange method, coupled with the newly introduced soft–core GB model can effectively speed–up equilibration of a GB liquid crystal phase by frequent exchange of configurations between replicas, while still recovering the mesogenic properties of the standard GB potential.

I. INTRODUCTION

Recent years have seen considerable interest in the simulation of liquid crystalline phases[1]. Model potentials have ranged from the simple ones used in lattice Hamiltonians[2], through hard and soft molecular (coarse–grained) models[3,4], to computationally demanding fully atomistic potentials[5,6]. Considerable understanding has been provided by coarse–grained models[3,4], which due to their relative simplicity, have allowed researchers to study molecular order, dynamics and bulk material properties in quite large scale simulations (> 1000 molecules) of a range of liquid crystalline phases[7]. Moreover, molecular potentials allow for the study of the properties of phases for which molecular structures are not yet available, and are thus invaluable in providing design hints to synthetic chemists, *e.g.* biaxial nematics[8] and ferroelectric nematics[9]. Very recently the possibility of simulating electro–optic devices, such as twisted nematic displays, has also been demonstrated using samples with $\approx 10^6$ GB particles[10].

In terms of computer time, molecular coarse–grained potentials, such as the Gay–Berne (GB) model[11], provide three key advantages over atomistic potentials. Most obvious is the speed–up in terms of a reduction in the number of sites relative to an atomistic model, albeit particle anisotropy is of course more demanding than spherically symmetric short–range interactions. However, almost as important is the increase in integration time–step that can be achieved in a molecular dynamics (MD) simulation, with the associated improvement in equilibration speed. Moreover, the very act of simplifying phase space, through which the sample moves, reduces the risk of evolution traps and speeds–up a calculation regardless of the chosen simulation technique[12,13].

For liquid crystalline systems, a major simulation cost is associated with taking a simulation through a phase transition to a more ordered phase. For instance, while gradually cooling–down an initially isotropic sample the spontaneous onset of an ordered domain, large enough to seed the formation of a stable liquid crystalline phase, requires long simulation times, due to the first order character of the isotropic–nematic (I-N) transition. The time for these ordering processes grows with system size and, even for relatively simple potential models, such as the GB, it is of considerable importance to speed–up these processes.

Problems of equilibration are ubiquitous in molecular simulations and have already received much attention. Amongst the many simulation strategies proposed to improve upon standard Monte Carlo and molecular dynamics approaches, are methods based on transition matrix Monte Carlo[14], Wang-Landau sampling[15,16], and new techniques such as Statistical

Temperature Molecular Dynamics[17–19]. The replica data methodology[20–22] has also become very popular and has been successfully employed for a range of systems. In its standard embodiment (*i.e.* parallel tempering), several MD simulations of similar samples are run concurrently at different temperatures. During the calculation many replica exchange Monte Carlo (MC) moves are attempted (either randomly or at regular intervals), each one trying to swap samples (*i.e.* particles and their coordinates) between two independent simulation runs at close temperatures using a Metropolis–like acceptance rule. The rationale behind this algorithm is that of improving configurational sampling at each temperature[23]. However, for hard particle or GB liquid crystals, parallel tempering bridging across an order–disorder phase transition is not a sensible option due to the exceedingly small acceptance ratio of configuration swap moves. In other words, the large distance in configuration space between the isotropic and the ordered phases means that it is very difficult to bridge temperatures embracing an order–disorder phase transition.

Another possibility which is attracting quite a large interest is to use Hamiltonian replica exchange MD (H–REMD)[24,25]. Here, it is the Hamiltonian of the system which is varied over the replicas, with replicas chosen in such a way that the barriers in the free energy landscape are smoothed out. The sampling of configuration space can thus become more efficient (*i.e.* faster). This leads to a significant speed–up in the equilibration of the unperturbed replica in comparison to conventional MD simulations, or to an easier escape from an otherwise kinetically–locked metastable state. Originally H–REMD was applied to proteins dissolved in implicit solvents or vacuum[25]. The results have shown that a scaled hydrophobicity led to a better sampling efficiency compared to standard replica exchange. H–REMD has also been used in simulations of biomolecules in explicit water[26,27], and recently was applied to studies of GTP and 8-Br-GTP molecules using soft–core interactions[28]. Key to the use of H–REMD is the availability of one or more interaction potentials to use in conjunction with the one of interest. Given our focus in liquid crystalline systems and the already mentioned relevance of GB potentials in the field, it is particularly important to devise a family of GB interactions that can reduce the risk of long–lived metastable states, *e.g.* by softening repulsion in the GB potential.

In this paper, we introduce a soft–core variant of the GB potential and show that, through the use of Hamiltonian replica exchange, this potential can be effectively used to speed–up the process of equilibration of a liquid crystalline phase and bypass metastable states.

II. SOFT–CORE GAY–BERNE MODEL

The model developed in this work is a soft–core variant of the standard Gay–Berne pair potential either in its standard form[11], or in its subsequent incarnations, *e.g.* biaxials[29–31], RE–squared[32,33], or the elliptic contact[34]. In this context, the label soft–core Gay–Berne (GBS) means that the $U^{GBS} < 0$ portion of the energy surface (corresponding to the centre–centre separation larger than the contact distance) is given by the GB potential U^{GB}, while the $U^{GBS} \geq 0$ branch is replaced with a functional term growing more slowly than the standard ones (*e.g.* $\propto r^{-12}$, or $\propto e^{-r}$) used to model the onset of short–range Pauli repulsions. Additionally, the soft–core term does not diverge to infinity for vanishing values of r, but takes a finite (possibly large compared to $k_B T$) value. This choice is reminiscent of the model potentials used in DPD simulations[35–37]. However, in our case, to maintain similarity between the phase diagrams for the soft–core and the standard models, the soft–core energy for $r = 0$ should be relatively large compared to $k_B T$.

The two energy surfaces are joined by a continuous switching function, which smoothly ranges from zero to one. The total energy between two soft–core ellipsoids is written as

$$U^{GBS} = [1 - f(r, \boldsymbol{\omega})]\, U^{GB}(r, \boldsymbol{\omega}) + f(r, \boldsymbol{\omega})\, U^{SC}(r, \boldsymbol{\omega}), \tag{1}$$

where the first term gives the standard GB contribution to the energy, while the second accounts for the soft–core repulsive barrier for distances smaller than contact between ellipsoids. To keep the notation compact (and general) the orientations for the two ellipsoids and the intermolecular vector are written as $\boldsymbol{\omega} \equiv (\boldsymbol{\omega}_1, \boldsymbol{\omega}_2, \boldsymbol{\omega}_r)$. The molecular orientations $\boldsymbol{\omega}_1$, $\boldsymbol{\omega}_2$ can be expressed as unit vectors if the ellipsoids are uniaxial, or as quaternions if biaxial. The intermolecular vector $\mathbf{r} = \mathbf{r}_2 - \mathbf{r}_1$ has length $r = \|\mathbf{r}\|$ and orientation $\boldsymbol{\omega}_r$. Forces and torques are easily computed from the derivatives $\mathbf{D}U^{GBS} = [1-f]\,\mathbf{D}U^{GB} + f\,\mathbf{D}U^{SC} + [U^{SC} - U^{GB}]\,\mathbf{D}f$, where $\mathbf{D}$ stands for the gradient $\nabla_{\mathbf{r}}$ or the angular momentum $\mathbf{L}_i$ operators.

The GB potential gives the interaction between two (possibly unlike[31]) ellipsoidal particles and can be written as

$$U^{GB}(r, \boldsymbol{\omega}) = 4\epsilon_0\, \epsilon(\boldsymbol{\omega}) \left[u^{12}(r, \boldsymbol{\omega}) - u^{6}(r, \boldsymbol{\omega})\right], \tag{2}$$

where $u(r, \boldsymbol{\omega}) = \sigma_c / (r - \sigma(\boldsymbol{\omega}) + \sigma_c)$ changes with the particle–particle distance r and the purely orientational contact term $\sigma(\boldsymbol{\omega})$, both measured in σ_0 units of length. The dimensionless anisotropic interaction term $\epsilon(\boldsymbol{\omega})$ controls the depth of the potential wells, while the ϵ_0 unit

defines the energy scale. Both $\sigma(\boldsymbol{\omega})$ and $\epsilon(\boldsymbol{\omega})$ are parameterised in terms of the axes σ_x, σ_y, and σ_z of the two ellipsoids. In addition, $\epsilon(\boldsymbol{\omega})$ also depends on the interaction coefficients ϵ_x, ϵ_y, and ϵ_z modelling the strength of the *side–by–side*, *face–to–face*, and *end–to–end* configurations[31]. Finally, the width and depth of the GB interaction wells can be tuned by means of the empirical parameters σ_c, μ, and ν. Explicit expressions for the anisotropic $\sigma(\boldsymbol{\omega})$, and $\epsilon(\boldsymbol{\omega})$ terms, as well for the forces and torques of the GB potential have been given elsewhere[38,39], and for concision will not be reported here.

The soft–core repulsive energy surface was modelled for every set of orientations $\boldsymbol{\omega}$ as a straight line with constant slope m passing through the locus $(\sigma(\boldsymbol{\omega}), 0)$ as

$$U^{SC}(r, \boldsymbol{\omega}) = m\,[r - \sigma(\boldsymbol{\omega})], \tag{3}$$

where $\sigma(\boldsymbol{\omega})$ is the anisotropic contact term of the GB potential. Using this prescription the whole surface of the GB ellipsoids has the same softness, *i.e.* the modulus of the soft–repulsive force between two overlapping particles does not depend on the particle–particle distance r since the gradient of the soft–core potential is

$$\nabla_{\mathbf{r}} U^{SC}(r, \boldsymbol{\omega}) = m\,[(\mathbf{r}/r) - \nabla_{\mathbf{r}}\sigma(\boldsymbol{\omega})]. \tag{4}$$

The soft–repulsive torques arising from U^{SC} can be computed after applying the angular momentum operators $\mathbf{L}_i$[38,39], and these also give purely orientational terms

$$\mathbf{L}_i U^{SC}(r, \boldsymbol{\omega}) = -m\,\mathbf{L}_i\sigma(\boldsymbol{\omega}). \qquad\qquad i = 1, 2 \tag{5}$$

Since these $\nabla_{\mathbf{r}}\sigma(\boldsymbol{\omega})$, and $\mathbf{L}_i\sigma(\boldsymbol{\omega})$ terms are routinely computed for the evaluation of the gradient and torques of the standard GB potential, the extension to the soft–core variant comes at a negligible extra computational cost, and requires minimal changes into existing MD (or MC) simulation codes.

The continuous blending between GB and soft–core potential surfaces was achieved by employing a logistic function $f(r, \boldsymbol{\omega})$ of sigmoidal shape

$$f(r, \boldsymbol{\omega}) = \exp[k\,(r - \sigma(\boldsymbol{\omega}))]/(1 + \exp[k\,(r - \sigma(\boldsymbol{\omega}))]). \tag{6}$$

The parameter k gives the *"steepness"* at the inflection point located at the anisotropic contact distance $r = \sigma(\boldsymbol{\omega})$. For $k < 0$ the switching function tends asymptotically to 0 for increasing values of r, while for $r < \sigma(\boldsymbol{\omega})$ it goes to unity. The slope k can be tuned to modulate the

steepness of the blending surface between U^{GB} and U^{SC}, *i.e.* to decrease (possible) undesirable oscillations in the repulsive force across the inflection point. If k is not small enough the U^{GB} branches diverging to infinity for r tending to 0 may not be cancelled out by the $1-f$ weight, and unwanted features in the total energy may appear for small particle–particle distances. In this case a (small) threshold value with respect to $1-f(r,\boldsymbol{\omega})$ can be introduced to cut–off this term to zero whenever $\|1-f\|$ is smaller than the threshold.

The gradient of the switching function is

$$\nabla_{\mathbf{r}} f(r,\boldsymbol{\omega}) = k\, f(r,\boldsymbol{\omega})[1-f(r,\boldsymbol{\omega})]\,[(\mathbf{r}/r) - \nabla_{\mathbf{r}}\sigma(\boldsymbol{\omega})], \tag{7}$$

while the effect of the angular momentum operators can be written as

$$\mathbf{L}_i f(r,\boldsymbol{\omega}) = -k\, f(r,\boldsymbol{\omega})[1-f(r,\boldsymbol{\omega})]\,\mathbf{L}_i\sigma(\boldsymbol{\omega}). \qquad i=1,2 \tag{8}$$

These expressions can also be used for modelling mixtures[31] of soft–core, or soft–core and standard particles, provided that interactions are computed using the parameterisation corresponding to the softest species of each pair.

As an example, in Figure 1 we report some representative energy profiles for the GBS potential plotted for the parameterisation $\sigma_x = \sigma_y = \sigma_c = \sigma_0$, $\sigma_z = 3\ \sigma_0$, and $\epsilon_x = \epsilon_y = \epsilon_0$, $\epsilon_z = 0.2\ \epsilon_0$, and $\mu = 1$, $\nu = 3$ of Ref.[7] (in short GB(3,5,1,3)), and with additional parameters $k = -100\ \sigma_0^{-1}$ and $m = -70\ \epsilon_0\sigma_0^{-1}$, for the steepness of the blending logistic function, and for the slope of the soft–core repulsion surface, respectively.

The soft GB interaction just introduced is of interest in its own right and will be studied in detail elsewhere[40]. Here, we only wish to verify if it leads to radically different phase behaviour with respect to the standard GB model, or if it can be used alongside it in the H–REMD procedure. To obtain this generic picture of the effects of softness on the mesogenic properties of a GB liquid crystal we have performed a preliminary exploration of the phase diagram of the GB(3,5,1,3) model. We have used MD simulations in the NVT ensemble with a velocity–Verlet integrator[41,42] and a weak–coupling Berendsen thermostat[43] to study an $N = 1024$ sample at dimensionless density $\rho^* \equiv N\sigma_0^3/V = 0.3$[7]. The time–step was $\Delta t^* = (\epsilon_0/\sigma_0^2 m_0)^{1/2}\Delta t = 0.001$, steepness $k = -70\ \sigma_0^{-1}$ and slope m ranged from $m = -100\ \epsilon_0\sigma_0^{-1}$ to $m = -20\ \epsilon_0\sigma_0^{-1}$. The results for the order parameter $\langle P_2\rangle = (1/\tau)\sum_t^\tau P_2(t)$ are given in Figure 2. The time average is computed with respect to the instantaneous $P_2(t) = (1/N)\sum_i^N [3(\mathbf{z}_i\cdot\mathbf{n})_t^2 - 1]/2$ giving the average orientation of long molecular axes $\mathbf{z}_i$ with respect to the configuration director $\mathbf{n}$[44]. We see that the steeper soft–repulsive energy barrier, $m = -60\ \epsilon_0\sigma_0^{-1}$, enhances the stability range

of ordered phases: the I-N transition shifts to a higher temperature. The soft–core samples also show larger values of the average order parameter, $\langle P_2 \rangle$, with respect to the standard GB over the entire temperature range. The weaker soft–repulsive barrier, $m = -30\ \epsilon_0 \sigma_0^{-1}$, impairs the anisotropy of the GB model: the I-N transition shifts to a lower temperature, and average $\langle P_2 \rangle$ values are now systematically lower. Finally, the intermediate barrier, $m = -40\ \epsilon_0 \sigma_0^{-1}$, closely follows the phase diagram of the standard GB in the smectic and nematic regions, and deviates only in giving a higher I-N transition temperature. These simulation results suggest that there are two competing effects with opposite influence on the mesogenic properties: (a) the softness allows an easier (lower energy) anisotropic close packing into mesogenic structures; and (b) softness also mellows the effective anisotropy of the potential by widening the area of the energy surface accessible at a given $k_B T$. The preliminary conclusion is that the potential energy softness can be effectively tuned to obtain both kind of order enhancing or depressing effects, or even to closely match the mesogenic properties of the standard GB model.

We note also that the soft–core coarse–grained potential used here has potential applications in its own right for the study of liquid crystalline systems, *e.g.* as a potential for the simulation of systems where the effective interaction range compared to particle size can be tuned, *e.g.* for anisotropic colloidal systems, or in view of bridging the mesoscopic gap between standard computer simulations and continuum techniques), or in a multi-site coarse–grained model for use with liquid crystalline macromolecules.

III. HAMILTONIAN REPLICA EXCHANGE

The Hamiltonian replica exchange algorithm[24,25] deploys several simulations running concurrently over a range of different (but relatively similar) Hamiltonians, corresponding to total potential energies $U_n(X_n)$, which are allowed to exchange the instantaneous state (*i.e.* coordinates) and swap the trajectory in phase (or configuration) space between pairs of contiguous runs.

In practice, the acceptance probability for the Hamiltonian exchange can be realised (see for example Refs.[25] and[26]) by considering two different replicas with energies $U_n(X_n)$ and $U_m(X_m)$ where X_n and X_m represent the configurational coordinates for the replicas n and m, respectively. The equilibrium probability (Boltzmann distribution) for the nth replica can

be written as

$$P_n = \frac{1}{Z_n} \exp\left[-\beta U_n(X_n)\right], \tag{9}$$

with $\beta \equiv 1/(k_B T)$. Now, considering the transition probability, $\Pi(X_n, U_n;\, X_m, U_m)$ that the configuration X_n in the nth replica exchanges with the configuration X_m in the mth replica, the detailed balance condition[42] can be written as

$$P_n(X_n)P_m(X_m)\Pi(X_n, U_n;\, X_m, U_m) = P_n(X_m)P_m(X_n)\Pi(X_m, U_n;\, X_n, U_m). \tag{10}$$

Substituting Equation 9 into Equation 10, the ratio of the transition probabilities can be obtained

$$\frac{\Pi(X_n, U_n;\, X_m, U_m)}{\Pi(X_m, U_n;\, X_n, U_m)} = \exp(-\Delta_{nm}), \tag{11}$$

where

$$\Delta_{nm} = \beta \left\{ [U_n(X_m) + U_m(X_n)] - [U_n(X_n) + U_m(X_m)] \right\}. \tag{12}$$

This yields a Metropolis–like acceptance criteria for the configuration exchange

$$\Pi(X_n, U_n;\, X_m, U_m) = \begin{cases} 1 & \text{if } \Delta_{nm} \leq 0, \\ \exp(-\Delta_{nm}) & \text{if } \Delta_{nm} > 0. \end{cases} \tag{13}$$

The sampling from this distribution is achieved by using the standard von Neumann rejection criterion. In our case we have simply two replicas: $U_0 = U^{GBS}$, and $U_1 = U^{GB}$.

IV. SIMULATION RESULTS

The MD simulations were performed using the parameterisation GB(3,5,1,3) (see Figure 1) together with $k = -100\ \sigma_0^{-1}$, and $m = -70\ \epsilon_0 \sigma_0^{-1}$ for the GBS potential. The threshold value for the logistic function was $\|1 - f\| = 10^{-6}$. The system consisted of $N = 1000$ particles in a cubic sample with periodic boundaries at dimensionless density $\rho^* \equiv N\sigma_0^3/V = 0.3$ which was simulated in the constant NVT ensemble using velocity rescaling to keep the dimensionless temperature constant to $T^* \equiv k_B T/\epsilon_0 = 2.8$. The equations of motions were integrated using the velocity–Verlet algorithm with dimensionless time–step of $\Delta t^* = 0.001$. For the standard GB(3,5,1,3) parameterisation the given state point is known to be well into the uniaxial nematic region with an order parameter $\langle P_2 \rangle \approx 0.82 \pm 0.01$[7]. The GBS system has instead a slightly higher orientational order $\langle P_2 \rangle \approx 0.85 \pm 0.01$ in agreement with the preliminary phase diagram results shown earlier.

Initial test benchmarks of the soft–core Hamiltonian exchange algorithm were performed using two replicas: one with ellipsoids interacting via the standard GB potential (equation 2), and the other with the GBS model (equation 1). All MD simulations used, as starting configurations, well–equilibrated GB isotropic samples at $T^* = 4.5$. Two different test cases of deep quenches of an initially isotropic sample brought to a temperature in the nematic region have been studied: one with both standard and GBS replicas using the same dimensionless time–step $\Delta t^*_{GB} = \Delta t^*_{GBS} = 0.001$; the other with a ten times larger time–step, $\Delta t^*_{GBS} = 0.01$, for the soft–core sample, and $\Delta t^*_{GB} = 0.001$. Attempts to exchange the configurations between the two replicas were carried out every 500, 100 or 50 MD time–steps using the acceptance criterion of Equation 13. To obtain an estimate of the average speed–up of the H–REMD equilibration with respect to the standard MD evolution a total of 20 independent H–REMD simulations were carried out in each case.

A comparison of the onset of the instantaneous orientational order parameter, P_2 (t), as a function of MD time–steps, at $T^* = 2.8$ for the H–REMD and for the standard GB simulations is presented in Figure 3. For the case where both replicas used the same time–step $\Delta t^* = 0.001$ (Figure 3–a) a speed–up of approximately 20% for equilibrating the nematic across the I-N phase transition was observed. Since the phase diagram for the two systems is similar, successful replica exchanges are frequent, and the standard GB sample thus benefits from the improved sampling.

To check the advantage of using longer time–steps in integrating the equations of motion for the soft–core potential, additional replica exchange simulations were run using the time–step $\Delta t^*_{GBS} = 0.01$ for the soft–core replica while attempting the exchange of configurations every $N_{ex} = 50$ or $N_{ex} = 100$ MD time–steps. We compared our H–REMD simulation results with those for standard GB simulations, where the onset of the nematic phase took place on average (considering ten independent equilibration runs) between 21000 MD time–steps in the best case and 45000 MD time–steps is the worst one. In the two H–REMD simulations cases a nematic order was achieved within a range of 3600–7600 and 4000–9600 MD time–steps, leading to speed–ups of approximately 2.8–12.5 and 2.2–11.3, for the systems with $N_{ex} = 50$ and $N_{ex} = 100$, respectively. (It must be noted that one of the MD simulation runs with $N_{ex} = 100$ failed to attain a stable nematic organisation within the 10000 MD time–steps window allowed for the experiments.) The acceptance probabilities for exchanging the replicas were $\Delta^{50}_{GBS-GB} \approx 0.212 \pm 0.006$ and $\Delta^{100}_{GBS-GB} \approx 0.23 \pm 0.01$.

In Figure 3–b an example of the time development of the orientational order parameter, P_2, is presented for the H–REMD system using a longer time–step $\Delta t^*_{GBS} = 0.01$ for the soft–core replica. An order of magnitude speed–up can be observed for the growth of a nematic phase for the GB replica. From the inset of the first 6000 MD time–steps of the simulation, Figure 3–c, the effectiveness of the replica exchange mechanism can be readily observed.

It is worth noting that while replica exchange works very well for speeding up nematic equilibration from an isotropic starting point, little (if any) speed–up is seen for the reverse process (regardless of the chosen value of m). This is mainly because formation of an isotropic is typically very rapid for Gay-Berne systems, and (unlike the nematic-isotropic case) does not suffer from slow growth of a uniform phase, after nucleation.

It is worth noting also that the choice of m in Figure 3 is not the optimum choice. (In this case $m = -70$ was chosen as a suitable value by noting the behaviour of the curves in Figure 1). In practice, as with other replica exchange approaches, it would be useful to carry out an initial (short) trial simulation to check the acceptance ratio for replica exchange swaps. If necessary m could be adjusted in the course of an initial "pre-production" part of a simulation. Indeed, it should be expected that the optimum choice of m will change with state point. Consequently, a useful extension of this methodology, involves taking advantage of several different replicas with different m parameters. Here, swaps are allowed between any randomly chosen pair. As an example, we present results for two state points, $T^* = 2.8$, $T^* = 3.4$, for a Gay-Berne with replicas corresponding to $m = -70$, $m = -80$ and $m = -160$. The lower part of figure 4 shows the acceptance ratios for the two runs for swaps involving each pair, with results averaged over 10 simulations each starting from independent configurations. In the case of the two temperatures shown, the balance of preferred swaps changes with state point. However, for both temperatures, the same set of replicas is able to speed up equilibration. For $T^* = 2.8$, the isotropic-nematic equilibration takes between 3300 and 6700 MD steps depending on the starting point (mean of 3965 MD steps over 10 independent simulations), and for $T^* = 3.4$ equilibration takes between 3730 and 6700 MD steps (mean of 4673 MD time steps). Unlike conventional parallel tempering the overlap between energy distributions is not the over-riding factor in determining the best acceptance ratio. The top part of figure 4 shows this by plotting histograms for the energy distribution within each of the four ensembles. The best direct overlap with the GB histogram occurs for the $m = -80$ replica. However, whether Δ (in equation 12) is sufficiently small (or negative) depends on the energy of the GB potential in

the $m = -80$ ensemble and vice versa. In the case of the system in figure 4, it is the $m = -160$ replica which fulfills this criteria best, i.e. $(U_n(X_n) - U_n(X_m)) \approx (U_m(X_n) - U_m(X_m))$ for a significant number of configurations (due to a balance between changes in attraction and repulsion between Hamiltonians), leading to efficient swapping with the GB system. As in the two-replica case, it would be possible to optimise m values by measuring the mean acceptance ratios during the initial stages of a simulation.

V. CONCLUSIONS

A simple soft–core family of Gay–Berne pair potentials (GBS) has been introduced, and a preliminary study of the effect of softness on the order parameters and phase behaviour of a system of uniaxial ellipsoidal particles interacting with this potential has been performed, finding that GBS interactions can be effectively varied to either increase or decrease mesogenic properties.

We have shown that by judicious choice of the softness of the repulsive region of the GBS potential a phase behaviour similar to that of the standard GB potential can be obtained, while preserving the relevant computational advantages stemming from the usage of longer time–steps, and reducing the risk of tangled configurations that are kinetically difficult to unlock.

We have also shown that, using this GBS potential in a Hamiltonian replica exchange MD (H–REMD) method can provide an effective way of significantly speeding–up equilibration for the standard GB potential that is known to provide a good representation of liquid crystalline organisations in a variety of systems[3,45]. We believe this to be particularly important as the scale of current simulations requires moving towards $\mathcal{O}(10^6)$ particle systems as required in simulations of devices[10] or of self–assembly[46], and that this GBS–GB H–REMD approach could provide a molecular based alternative to DPD–like methods.

VI. ACKNOWLEDGEMENTS

RB and CZ thank the EU–STREP project *"Biaxial Nematic Devices"* (BIND) FP7–216025 for financial support. JSL thanks the HPC–Europa2 project for a grant, and the CINECA

computing centre for computer time.

---

[1] M. R. Wilson, Int. Rev. Phys. Chem. **24**, 421 (2005).

[2] P. Pasini and C. Zannoni, editors, *Advances in the Computer Simulation of Liquid Crystals* (Kluwer, Dordrecht, 1999), 1st ed.

[3] C. Zannoni, J. Mater. Chem. **11**, 2637 (2001).

[4] C. M. Care and D. J. Cleaver, Reports on Progress in Physics **68**, 2665 (2005).

[5] M. R. Wilson, Chem. Soc. Rev. **36**, 1881 (2007).

[6] G. Tiberio, L. Muccioli, R. Berardi and C. Zannoni, ChemPhysChem **10**, 125 (2009).

[7] R. Berardi, A. P. J. Emerson and C. Zannoni, J. Chem. Soc., Faraday Trans. **89**, 4069 (1993).

[8] R. Berardi and C. Zannoni, J. Chem. Phys. **113**, 5971 (2000).

[9] R. Berardi, M. Ricci and C. Zannoni, ChemPhysChem **2**, 443 (2001).

[10] M. Ricci, M. Mazzeo, R. Berardi, P. Pasini and C. Zannoni, Faraday Discuss. **144**, *in press* (2009).

[11] J. G. Gay and B. J. Berne, J. Chem. Phys. **74**, 3316 (1981).

[12] J. S. Lintuvuori and M. R. Wilson, J. Chem. Phys. **128**, 044906.1 (2008).

[13] Z. E. Hughes, L. M. Stimson, H. Slim, J. S. Lintuvuori, J. M. Ilnytskyi and M. R. Wilson, Comp. Phys. Comm. **178**, 724 (2008).

[14] J. R. Errington, J. Chem. Phys. **118**, 9915 (2003).

[15] F. G. Wang and D. P. Landau, Phys. Rev. Lett. **86**, 2050 (2001).

[16] M. S. Shell, P. G. Debenedetti and A. Z. Panagiotopoulos, J. Chem. Phys. **119**, 9406 (2003).

[17] J. Kim, J. E. Straub and T. Keyes, Phys. Rev. Lett. **97**, 050601 (2006).

[18] J. Kim, J. E. Straub and T. Keyes, J. Chem. Phys. **126** (2007).

[19] J. Kim, T. Keyes and J. E. Straub, J. Chem. Phys. **130** (2009).

[20] D. J. Earl and M. W. Deem, Phys. Chem. Chem. Phys. **7**, 3910 (2005).

[21] C. Y. Lin, C. K. Hu and U. H. E. Hansmann, Proteins **52**, 436 (2003).

[22] U. H. E. Hansmann, Chem. Phys. Lett. **281**, 140 (1997).

[23] H. A. Slim and M. R. Wilson, J Chem. Theory Comput. **4**, 1570 (2008).

[24] Y. Sugita, A. Kitao and Y. Okamoto, J Chem. Phys. **113**, 6042 (2000).

[25] H. Fukunishi, O. Watanabe and S. Takada, J. Chem. Phys. **116**, 9058 (2002).

[26] P. Liu, B. Kim, R. A. Friesner and B. J. Berne, Proc. Natl. Acad. Sci. **102**, 13749 (2005).

[27] R. Affentranger, I. Tavernelli and E. E. Di Iorio, J. Chem. Theory Comput. **2**, 217 (2006).

[28] J. Hritz and C. Oostenbrink, J. Chem. Phys. **128**, 144121.1 (2008).

[29] R. Berardi, C. Fava and C. Zannoni, Chem. Phys. Lett. **236**, 462 (1995).

[30] D. J. Cleaver, C. M. Care, M. P. Allen and M. P. Neal, Phys. Rev. E **54**, 559 (1996).

[31] R. Berardi, C. Fava and C. Zannoni, Chem. Phys. Lett. **297**, 8 (1998).

[32] R. Everaers and M. R. Ejtehadi, Phys. Rev. E **67**, 041710 (2003).

[33] M. Babadi, R. Everaers and M. R. Ejtehadi, J. Chem. Phys. **124**, 174708 (2006).

[34] L. Paramonov and S. N. Yaliraki, J. Chem. Phys. **123**, 194111.1 (2005).

[35] P. J. Hoogerbrugge and J. M. V. A. Koelman, Europhys. Lett. **19**, 155 (1992).

[36] J. M. V. A. Koelman and P. J. Hoogerbrugge, Europhys. Lett. **21**, 363 (1993).

[37] P. Espanol and P. Warren, Europhys. Lett. **30**, 191 (1995).

[38] M. P. Allen and G. Germano, Mol. Phys. **104**, 3225 (2006).

[39] R. Berardi, L. Muccioli and C. Zannoni, J. Chem. Phys. **128**, 024905.1 (2008).

[40] R. Berardi, J. S. Lintuvuori, M. R. Wilson and C. Zannoni, *to be published* (2009).

[41] M. P. Allen and D. J. Tildesley, *Computer Simulation of Liquids* (Oxford University Press, 1989).

[42] D. Frenkel and B. Smit, *Understanding Molecular Simulations: From Algorithms to Applications, 2nd edition* (Academic Press, 2001).

[43] H. J. C. Berendsen, J. P. M. Postma, W. F. van Gunsteren, A. DiNola and J. R. Haak, J. Chem. Phys. **81**, 3684 (1984).

[44] C. Zannoni, in *Nuclear Magnetic Resonance of Liquid Crystals*, edited by J. Emsley, chap. 1, 1–34 (Reidel, Dordrecht, The Netherlands, 1985).

[45] R. Berardi, L. Muccioli, S. Orlandi, M. Ricci and C. Zannoni, J. Phys.: Condens. Matter **20**, 463101.1 (2008).

[46] M. L. Klein and W. Shinoda, Science **321**, 798 (2008).

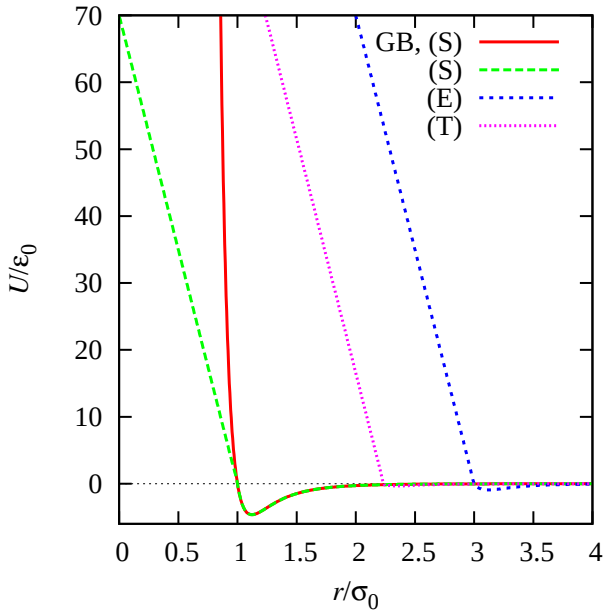

FIG. 1: Representative profiles for the soft–core Gay–Berne potential with $\sigma_x = \sigma_y = \sigma_c = 1\ \sigma_0$, $\sigma_z = 3\ \sigma_0$, and $\epsilon_x = \epsilon_y = 1\ \epsilon_0$, $\epsilon_z = 0.2\ \epsilon_0$, and $\mu = 1$, $\nu = 3$, and steepness $k = -100\ \sigma_0^{-1}$, and slope $m = -70\ \epsilon_0\sigma_0^{-1}$. The threshold value for the logistic function cut–off was $\|1 - f\| = 10^{-6}$. The energy curves are relative to three specific configurations: *side–by–side* (S), *tee* (T), and *end–to–end* (E). A plot for the standard GB *side–by–side* interaction energy is also provided for comparison.

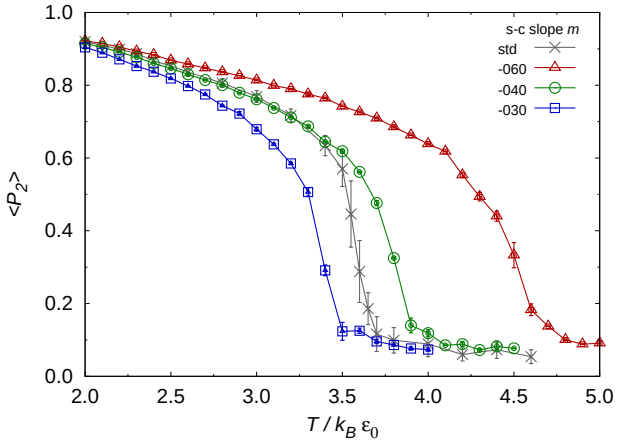

FIG. 2: The orientational order parameter $\langle P_2 \rangle$ for the soft–core GB potential parameterisation described in the text with logistic function steepness $k = -100\ \sigma_0^{-1}$, and soft–core slopes $m = -60$, -40, and $-30\ \epsilon_0 \sigma_0^{-1}$. The state points are from MD simulations in the NVT ensemble for an $N = 1024$ sample at dimensionless density $\rho^* = 0.3$. The reference points from the NVT simulation of the standard GB(3,5,1,3) model[7] are given by grey points.

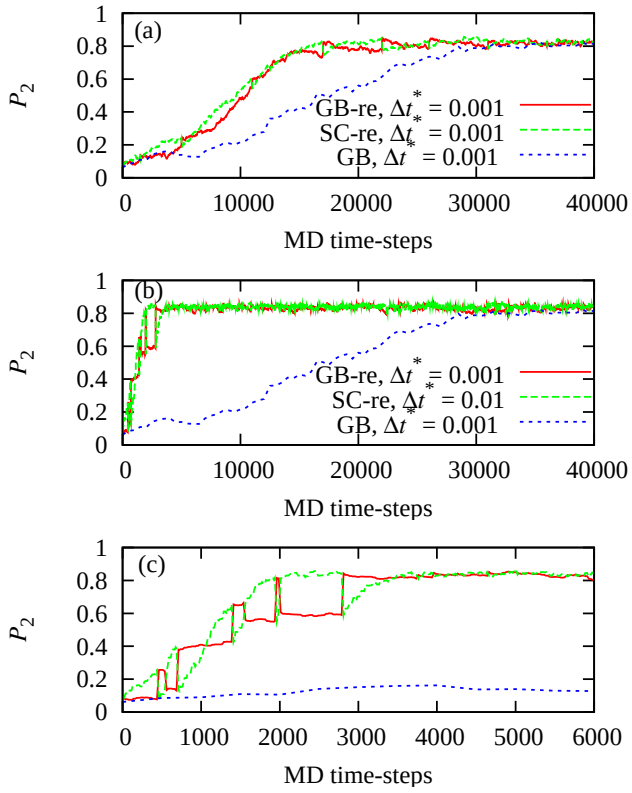

FIG. 3: The instantaneous order parameter P_2 for the Hamiltonian replica exchange benchmark simulations. Bold line GB replica; dashed line GBS replica; dotted line standard GB simulation with $\Delta t^* = 0.001$ (provided for comparison). Plate (a) both GB and GBS replicas are run with same time–step $\Delta t^*_{GBS} = \Delta t^*_{GB} = 0.001$; plate (b) GBS replica with time–step $\Delta t^*_{GBS} = 0.01$, and GB replica with $\Delta t^*_{GB} = 0.001$; and plate (c) enlargement of the first 6000 MD time–steps from the system with $\Delta t^*_{GBS} = 0.01$ and $\Delta t^*_{GB} = 0.001$ of plate (b).

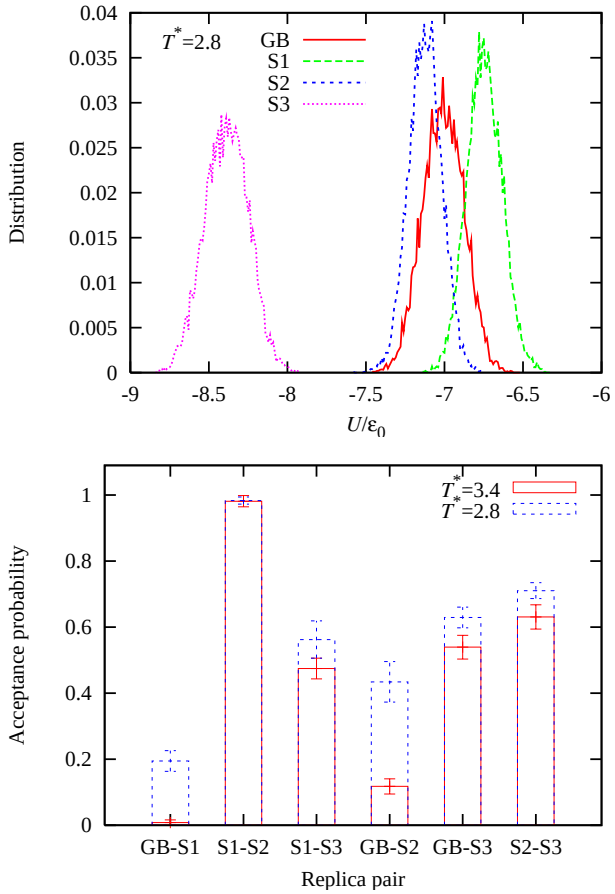

FIG. 4: Top: Distribution of energies for 4 replicas (GB, S1 ($m = -70$), S2 ($m = -80$), (S3) $m = -160$) for simulations at $T^* = 2.8$. Bottom: Acceptance probabilities at $T^* = 2.8$ and $T^* = 3.4$ for replica exchanges between GB, S1, S2, and S3 ensembles.